

The behavior of amorphous alloys under swift heavy ion irradiation at room temperature

Alexander Yu. Didyk,
Andrzej Hofman,
Valeriy V. Savin,
Vera K. Semina,
Ewa Hajewska,
Witold Szteke,
Wojciech Starosta

Abstract Experimental results of irradiation effects by heavy ions with high inelastic energy losses at the surfaces of some amorphous alloys are presented. It was shown that all studied alloys strongly swelled: up to 15% for $\text{Ni}_{58}\text{Nb}_{42}$ under irradiation with the 305 MeV ^{86}Kr ion at a fluence of 10^{15} ion/cm². Besides, the sputtering (evaporation) process takes place, too. Calculations of the temperatures on the ion trajectory axis were presented. It was shown that the calculated temperatures are higher than the melting temperature and the evaporation temperature, too. From these findings we can conclude that the sputtering (evaporation) of atoms in amorphous alloys is present.

Key words amorphous alloy • heavy ion irradiation • sputtering • surface structure • swelling

Introduction

It is interesting to study the interaction of swift heavy ions with metals, alloys and amorphous alloys. Studying on structural changes and other properties of amorphous metal alloys irradiated with swift heavy ions in the high inelastic energy loss region is important for a number of reasons. First of all, such systems do not have a long-range order in atomic arrangement and exhibit only a short-range order. Amorphous systems are disordered materials, and thus investigations of amorphous alloys attract interest for several reasons [1, 8–10, 13, 15, 18, 25]. The main published results are as follows:

1. Under irradiation with heavy ions, the dimensions of samples perpendicular to ion beam direction increased, but the sample dimension along the ion beam shrunk.
2. The processes of sputtering were strongly suppressed.
3. These irradiation-induced dimension changes were not accompanied with volume changes.

The purpose of this article was to study the radiation phenomena in amorphous alloys such as $\text{Ni}_{58}\text{Nb}_{42}$, $\text{Fe}_{77}\text{Ni}_2\text{Si}_{14}\text{B}_7$ and $\text{Ta}_{37}\text{Ni}_{63}$ under the influence of high fluences of swift heavy ions [21, 22].

Experimental results with amorphous alloys under irradiation with swift heavy ions and discussions of a model

The samples of amorphous alloys $\text{Ni}_{58}\text{Nb}_{42}$, $\text{Fe}_{77}\text{Ni}_2\text{Si}_{14}\text{B}_7$ and $\text{Ta}_{37}\text{Ni}_{63}$ were irradiated with 245 MeV ^{84}Kr ions up to the fluences 10^{14} and 10^{15} ion/cm² and

A. Yu. Didyk✉, A. Hofman, V. K. Semina
Joint Institute for Nuclear Research, FLNR,
141980 Dubna, Russia,
Tel.: +7 09621 63376, Fax: +7 09621 65955,
E-mail: didyk52@mail.ru; didyk@jinr.ru

V. V. Savin
Zaporizhzhya State University,
66 Zhukovskiy Str., Ukraine 69600 Zaporizhzhya

E. Hajewska, W. Szteke
Material Research Laboratory Department,
Institute of Atomic Energy,
05-400 Otwock-Świerk, Poland

W. Starosta
Institute of Nuclear Chemistry and Technology,
16 Dorodna Str., 03-195 Warsaw, Poland

Received: 30 November 2004
Accepted: 11 October 2005

710 MeV ^{209}Bi ions up to the fluences 10^{12} and 10^{13} ion/cm 2 . The irradiation temperature was less than 100°C. The irradiation was carried out using the set-up described in Refs. [20, 23]. The mean flux of ion beam was $F \sim 10^{11}$ ion/(cm 2 ·s) and less.

The initial surface of $\text{Ni}_{58}\text{Nb}_{42}$ sample is presented in Fig. 1a. One can see the defects of surface structure – the frozen melt drops.

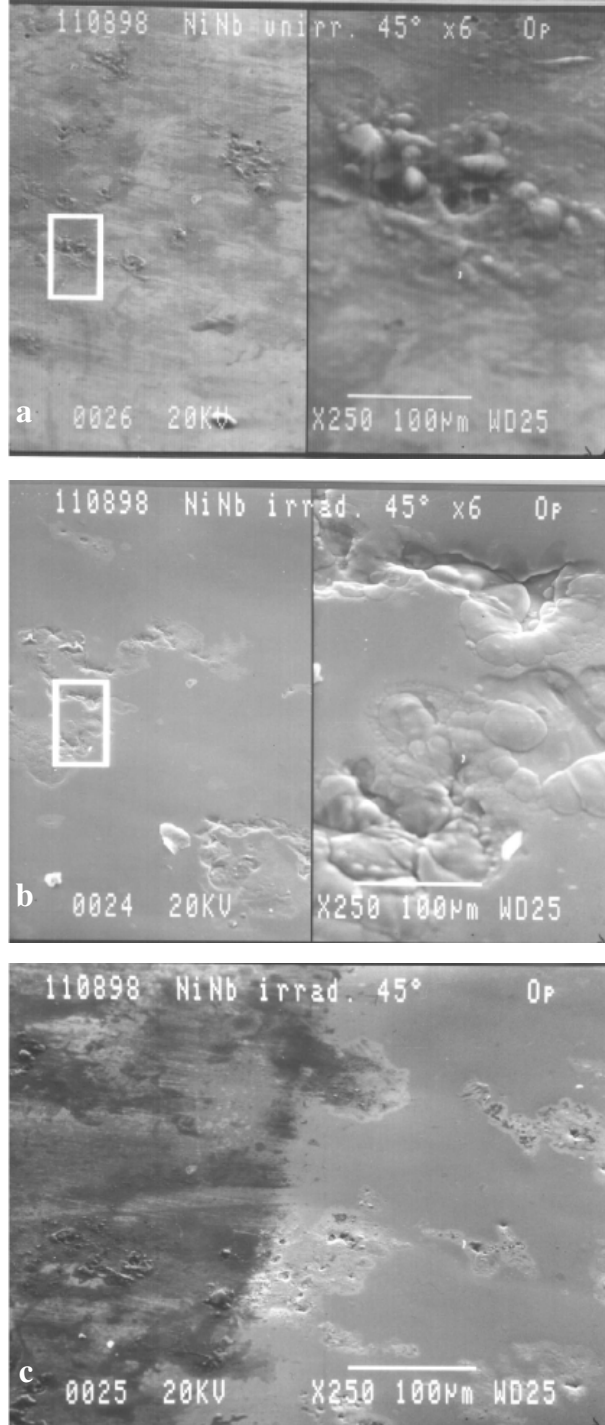


Fig. 1. The amorphous $\text{Ni}_{58}\text{Nb}_{42}$ alloy surface structure: a – unirradiated; b – irradiated with 245 MeV ^{86}Kr ions up to the fluence $F \cdot t = 1 \times 10^{15}$ ion/cm 2 ; and c – is the structure of the sample partially masked by a foil (on the left is the unirradiated region and on the right – the irradiated one).

The surface structures of irradiated amorphous $\text{Ni}_{58}\text{Nb}_{42}$ are presented in Figs. 1b and 1c. One can see that at the temperature $T \approx 300$ K the sample surface changed very strongly. The areas with the frozen melt drops practically kept the position on the surface, but the relatively smooth area around these drops was displaced along the ion bombardment direction so that the drops became immersed under the smooth surface part. The swelling value of samples irradiated with 245 MeV ^{86}Kr ions at a fluence of $F \cdot t = 10^{15}$ ion/cm 2 was found to be $\Delta V/V \sim 15\%$. The chemical composition on the sample surface was found to change, too. The chemical composition of the alloy can be expressed as $\text{Ni}_{58-x}\text{Nb}_{42+x}$, where $x = 1.60$ at an ion fluence of $F \cdot t = 10^{15}$ ion/cm 2 and $x = 1.48$ at an ion fluence of $F \cdot t = 10^{14}$ ion/cm 2 . One can conclude that the significant changes of chemical composition at relatively low fluences must be caused by evaporation processes rather of Ni than Nb atom as the latter is a more refractory element.

In Fig. 2 the $\text{Ni}_{58}\text{Nb}_{42}$ surface structures obtained by scanning tunneling microscopy (STM) are presented. One can see that the volume increase is connected with the multistep volume growth, but not with surface growth. The projected range of ^{86}Kr ions in $\text{Ni}_{58}\text{Nb}_{42}$ alloy is $R_p = 13.4$ μm (the density of this alloy is $\rho_i = 8.54$ g/cm 3 , the threshold energy for damage creation being $E_{td} \approx 30$ eV). The inelastic energy loss is $(dE/dx)_{inel} = 23.84$ MeV/ μm and the damage doses created in the process of elastic collisions are $\sigma_{el}(F \cdot t) = 0.037$ dpa and $\sigma_{el}(F \cdot t) = 0.0037$ dpa for the ^{86}Kr ion fluences 10^{15} and 10^{14} ion/cm 2 , respectively. The cross section of a target atom displacement for the interaction $\text{Ni}_{58}\text{Nb}_{42}$ with ^{86}Kr is $\sigma_{el} = 3.7 \times 10^{-17}$ dpa·cm 2 /ion. The parameters $S_e = (dE/dx)_{inel} \cdot R_p$ and σ_{el} were estimated by means of a computer code SRIM.

The temperature values ($T_{tr} > T_{melt}$) can be calculated from a simple expression for temperature calculations presented in [2, 3] and is based on the calculated S_{inel} values:

$$(1) \quad T_{tr} = \frac{S_{inel}(x)}{\pi R_{tr}^2 C_i \rho_i} + T_{initial}$$

So, according to expression (1) the temperature on the ion track axis will be about $T_{tr} \sim 1.6 \times 10^4$ K. For the estimation of time dependence of temperature in the area around ion trajectory, we used the following expression [16, 19]:

$$(2) \quad T_{tr}(t) = \frac{S_{inel}}{4\pi\zeta t} \cdot \exp\left(-\frac{C_V r^2}{4\zeta t}\right) + T_{initial}$$

In expressions (1) and (2), C_i is the specific heat capacity in J/(kg·K); ρ_i is the material density; R_{tr} is the track radius; T_0 is the irradiation temperature; C_V is the specific heat capacity in kJ/(m 3 ·K); $C_V = C_i \cdot \rho_i$; ζ is the heat conductivity coefficient in W/(m·K). The calculation of temperature T_{tr} was carried out using expression (1) for the parameters: $R_{tr} \sim 50$ Å, $C_i \approx 368$ J/(kg·K), $\rho_i = 8540$ kg/m 3 , $\zeta = 54$ W/(m·K).

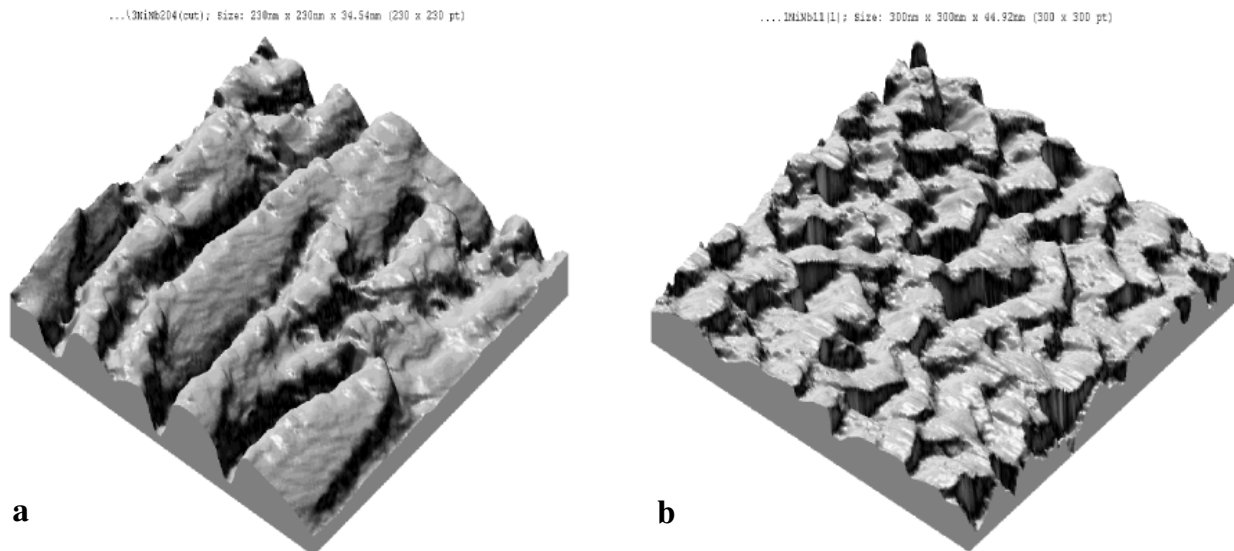


Fig. 2. The structure of amorphous $\text{Ni}_{58}\text{Nb}_{42}$ alloy irradiated with 245 MeV ^{86}Kr ions up to the fluence $F \cdot t = 1 \times 10^{15}$ ion/cm² (b – 300 nm × 300 nm × 44.92 nm) and unirradiated (a – 230 nm × 230 nm × 34.54 nm).

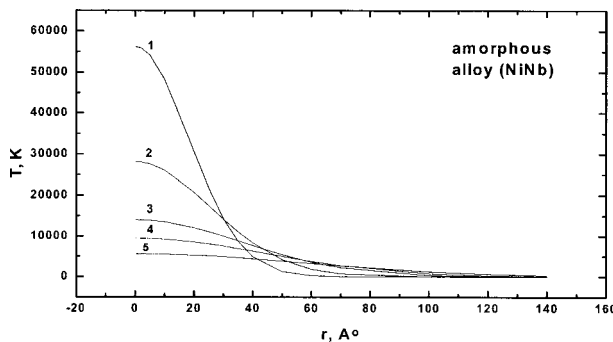


Fig. 3. The temperature as a function of the distance r from the 245 MeV ^{86}Kr ion trajectory axis for various times: 1 – $t_1 = 1 \times 10^{-13}$ s; 2 – $t_2 = 2 \times 10^{-13}$ s; 3 – $t_3 = 4 \times 10^{-13}$ s; 4 – $t_4 = 6 \times 10^{-13}$ s and 5 – $t_5 = 10^{-12}$ s.

Figure 3 shows the temperature as a function of the distance from the heavy ion trajectory axis (r) for various times after ion passing: $t_1 = 10^{-13}$ s, $t_2 = 2 \times 10^{-13}$ s, $t_3 = 4 \times 10^{-13}$ s, $t_4 = 6 \times 10^{-13}$ s and $t_5 = 10^{-12}$ s.

The time dependence of the temperature on the track axis after ^{86}Kr ion passing through the $\text{Ni}_{58}\text{Nb}_{42}$ alloy can be written as

$$(3) \quad T_r(t, r = 0) = 5.62 \times 10^4 \cdot t_1/t_2$$

One can see that the full width at a half maximum of temperature distribution for $t_1 = 10^{-13}$ s is $R_r \approx 25$ Å. So, if we will take this value instead of $R_r \sim 50$ Å in Eq. (1), the estimated temperature must be $T_r \sim 4 \times 1.6 \times 10^4$ K = 6.4×10^4 K. The value is practically the same as the values at $r = 0$ and $t_1 = 10^{-13}$ s which are presented in Fig. 3.

The pressure in the area around the hot ion track with the temperature $T_r \sim 10^4$ K (without changes of volume) must be approximately 10^2 kbar (see [14, p. 249]). So, the target atoms can be thrown out from the surface by high pressure, too.

The time and distance dependence of temperature around ion track is calculated using the expressions from

some publications [8, 17, 24]. The temperature peak (thermal spike) model was used for description of radiation phenomena under irradiation with swift heavy ions of solids (e.g. [24]). These model calculations are based on earlier publications [7, 17]. The expressions, which were obtained in these works, have the form

$$(4a) \quad C_e \frac{dT_e}{dt} = \frac{1}{r} \frac{d}{dr} \left(r K_e \cdot \frac{dT_e}{dr} \right) - \alpha (T_e - T_i) + A(\rho, t)$$

$$(4b) \quad C_i \frac{dT_i}{dt} = \frac{1}{r} \frac{d}{dr} \left(r K_i \cdot \frac{dT_i}{dr} \right) + \alpha (T_e - T_i)$$

Here C_e and C_i are the specific heat capacities for electrons and lattice atoms, and K_e and K_i are the electronic and lattice thermal conductivities, respectively; C and K are the temperature-dependent parameters; α is the constant of electron-phonon interaction.

The use of expressions (1), (2) and (4) allows one to estimate the temperature on the axis of Kr ion track in amorphous alloys. The temperature of the ion track near the axis, T_r , is higher than the melting point and the evaporation temperature for this $\text{Ni}_{58}\text{Nb}_{42}$ amorphous alloy. This follows from all these expressions. So, in this material the evaporation (sputtering) processes must take place.

Discussion and conclusion

The presence of the developed defect structure in amorphous metal alloys essentially increases the influence of inelastic energy losses of fast heavy ions on the sputtering yield and changes of structural properties such as swelling. This is connected with the decrease of the free paths of electrons. Therefore, the energy from “hot” electrons cannot dissipate on

large distances from the ion axis. Thus, a thermal peak model should work at such systems and the temperature on the ion track will be much higher than the melting and evaporation temperature for amorphous alloys. The hot electron plasma model [26] does not contradict the experimental results presented in this work.

The scanning electron microscopy studies show that the frozen melt drops did not change the position on the surface and turned out to immerse into a swelling surface as the “islands of inhomogeneity”. The swelling value of samples irradiated at room temperature with 245 MeV ^{86}Kr ions at $F \cdot t \sim 10^{14}$ – 10^{15} ion/cm² is found to be very high. The sputtering of $\text{Ni}_{58}\text{Nb}_{42}$ also takes place, and changes of the surface elemental composition were observed.

The conclusion on the influence of defects on temperature in the volume around ion track is proved by the results of the studies [5, 6] on track formation in a single-crystal InP semiconductor irradiated previously with 5 MeV electrons (fluence 5×10^{17} electron/cm²) and then with 250 and 340 MeV ^{129}Xe and 245 and 210 MeV ^{86}Kr ions. Heavy ion tracks were also found in amorphous Si and Ge [4]. The processes of damage concentration saturation in some materials (like Ge, C, W etc.) as a function of the swift heavy ion fluence were observed in a set of publications (see, e.g. [11]). A model of disordering and following crystal recrystallization under heavy ion irradiation was developed in Ref. [12].

The importance of the sputtering problem for accelerator engineering and for high-energy heavy ion implantation into up-to-date materials is evident. To understand the observed phenomena it is necessary to continue the study on radiation effects in various amorphous alloys under irradiation with swift heavy ions and fast ($E_n > 0.1$ MeV) neutrons.

References

- Audouard A, Balanzat E, Jousset JC, Lesueur D, Thomé L (1995) Atomic displacements and atomic motion induced by electron excitation in heavy-ion-irradiated amorphous metallic alloys. *J Phys-Condens Matter* 5:995–1018
- Davydov AA, Kalinichenko AI (1985) Mechanical effects near ion tracks and thermal peaks. *Voprosy Atomnoj Nauki i Tekhniki. Radiation Damage Physics and Radiation Technology (Rus)* 3;36:27–30
- Didyk AYU (1995) Heavy ion irradiation effect on chromium-nickel steel at high temperatures. *Metally (Rus)* 3:128–135
- Furuno S, Otsu H, Hojou K, Izui K (1996) Tracks of high-energy heavy ions in solids. *Nucl Instrum Meth Phys Res B* 107:223–226
- Gaiduk PI, Komarov FF, Tishkov VS, Wesch W, Wendler E (2000) Wurtzite InP formation during swift Xe-ion irradiation. *Phys Rev B* 61:15785–15788
- Gaiduk PI, Komarov FF, Wesch W (2000) Damage evolution in crystalline InP during irradiation with swift Xe ions. *Nucl Instrum Meth Phys Res B* 164/165:377–383
- Gegusin YaE, Kaganov MI, Lifshic IM (1973) Electron free length effect on track formation around charged particle trajectory in metal. *Fizika Tverdogo Tela (Rus)* 15:2425–2428
- Gutzmann A, Klaumünzer S (1997) Shape instability of amorphous materials during high-energy ion bombardment. *Nucl Instrum Meth Phys Res B* 127/128:12–17
- Gutzmann A, Klaumünzer S, Meier P (1995) Ion-beam-induced surface instability of glassy $\text{Fe}_{40}\text{Ni}_{40}\text{B}_{20}$. *Phys Rev Lett* 74:2256–2259
- Hou Ming-Dong, Klaumünzer S, Schumacher G (1990) Directional changes of metallic glasses during bombardment with fast heavy ions. *Phys Rev B* 41:1144–1157
- Huber H, Assmann W, Karamian SA *et al.* (1998) Heavy-ion induced damage of crystalline Ge and W in the 0.5–8 A MeV range. *Nucl Instrum Meth Phys Res B* 146:309–316
- Karamian SA, Oganessian YuTs, Bugrov VN (1989) The effect of high-energy ions heavier than argon on a germanium single crystal and a new mechanism for autore-crystallisation. *Nucl Instrum Meth Phys Res B* 43:153–158
- Klaumünzer S (2000) Radiation compaction of porous Vycor glass. *Nucl Instrum Meth Phys Res B* 166/167:459–464
- Komarov FF, Novikov AP, Burenkov AF (1994) Ion implantation. Minsk University, Minsk (in Russian)
- Kuch H, Klaumünzer S (1998) Magneto-optical study of flux-line pinning in semiconductors with linear defects. *Nucl Instrum Meth Phys Res B* 146:565–571
- Kulikov DV, Suvorov AL, Suric PA, Trushin YuV, Kharlamov VS (1997) Physical model of formation periodical structure on the surface of pyrolytic graphite at high energy ion irradiation. *Let J Tech Phys (Rus)* 23;14:89–93
- Lifshic IM, Kaganov MI, Tanatarov LV (1959) On the theory of radiation changes in metals. *Atomnaja Energija (Rus)* 6:391–402
- Meftah A, Djebara M, Khalfaoui N, Toulemonde M (1998) Sputtering of vitreous SiO_2 and $\text{Y}_3\text{Fe}_5\text{O}_{12}$ in the electronic stopping power region: A thermal spike description. *Nucl Instrum Meth Phys Res B* 46:431–436
- Nastasi M, Mayer JW (1994) Ion beam mixing and liquid interdiffusion. *Radiat Eff Defects Solids* 130/131:367–385
- Oganessian YuTs, Dmitriev SN, Didyk AYU, Gulbikian GG, Kutner VB (2000) New possibilities of the FLNR accelerator complex for the production of track membranes. In: *Proc of the 10th Int Conf Radiation Physics of Solids, Sevastopol, Ukraine*, pp 42–50
- Semina VK, Didyk AYU, Altynov VA (2001) The changes in amorphous alloy under high-energy heavy ions irradiation. In: *Proc of the 6th Int Seminar: Structural principles of material modifications by unconventional technologies, Obninsk, Russia*, pp 24–25 (in Russian)
- Semina VK, Didyk AYU, Altynov VA *et al.* (2001) Structural changes in amorphous alloys under irradiation with high energy heavy ions. In: *Proc of the 11th Int Conf Radiation Physics of Solids, Sevastopol, Ukraine*, pp 10–15 (in Russian)
- Skuratov VA, Illes A, Illes Z *et al.* (1999) Beam diagnostics and data acquisition system for ion beam transport line used in applied research. *JINR Communications* E13-99-161. JINR, Dubna
- Toulemonde M (1999) Nanometric phase transformation of oxide materials under GeV energy heavy ion irradiation. *Nucl Instrum Meth Phys Res B* 156:1–11
- Trautmann C, Dufour C, Paumier E, Spohr R, Toulemonde M (1996) Track etching in amorphous metallic $\text{Fe}_{81}\text{B}_{13.5}\text{Si}_{3.5}\text{C}_2$. *Nucl Instrum Meth Phys Res B* 107:397–402
- Yavlinskii YuN (2000) Heating of crystalline and amorphous metals under swift heavy-ion irradiation. *Radiat Eff Defects Solids* 153:75–91